IUST
Iran University of Science and Technology

Iranian Journal of Electrical and Electronic Engineering

Journal Homepage: ijeee.iust.ac.ir

Design of a High-Efficiency Dynamic Wireless Charger for Electric Vehicles

Majid Moghaddam*(C.A.)

Abstract: The widespread adoption of electric vehicles (EVs) is hindered by battery-related limitations, including high cost, excessive weight, long charging times, and insufficient charging infrastructure. This study presents an inductive wireless power transfer (WPT) system as a practical step toward dynamic wireless power transfer (DWPT), aiming to reduce the required onboard battery capacity and weight. The proposed system employs an H-bridge inverter with sinusoidal pulse width modulation (SPWM). A three-phase diode bridge rectifier followed by an active power factor correction (PFC) boost converter with zero-voltage switching (ZVS) converts the three-phase AC input into a 600 V DC link. The switching frequency is optimized at 100 kHz to minimize losses and maximize power transfer efficiency. Both air-core and ferrite-core coil configurations are simulated and modelled with an approximate 10 cm air gap, representing the typical clearance between the road and the EV underbody. The system wirelessly transfers 2.4 kW of power to the EV, achieving a coil-to-coil efficiency exceeding 96%. The received high-frequency AC power is then rectified and smoothed by a synchronous rectifier and an LC output filter, delivering a stable 200 V DC output suitable for constant-current/constant-voltage (CC-CV) charging of the EV battery pack. The results confirm the feasibility of in-motion wireless charging as a practical solution to key EV limitations.

Keywords: Electric Vehicle, Wireless Power Transfer, Dynamic Wireless Power Transfer, Inductive Power Transfer, Coil-to-Coil Efficiency.

1 Introduction

THE global reliance on fossil fuels presents a multidimensional security challenge, encompassing geopolitical instability, economic volatility, and infrastructure vulnerability. Whereas, fossil fuel demand is projected to grow minimally, the nature of energy security risks is shifting toward structural pressures in energy systems and supply chains. This reliance, particularly on crude oil, coupled with the severe environmental consequences of greenhouse gas and particulate emissions from key sectors such as transportation, industry, and power generation, constitutes a pressing dual crisis [1], [2]. Low-power design is now a major challenge, especially for battery-operated systems. Portable devices require extremely low power consumption to prolong battery life, making this a key focus in modern electronics [3]-[5].

In response, the international community is increasingly prioritizing the reduction of fossil fuel consumption and its replacement with clean, low-carbon energy carriers.

Within this energy transition, Electric Vehicles (EVs) have emerged as one of the most promising solutions for the transportation sector. Their demand is experiencing exponential growth, driven by heightened environmental awareness and parallel advancements in two critical technologies: high-energy-density lithium-ion batteries and rapid, efficient charging systems [6], [7]. The electrification of transport fleets offers a strategic pathway to decouple this sector from oil, linking it

Iranian Journal of Electrical & Electronic Engineering, 2026.
Paper first received 23 Jan 2026 and accepted 23 Aug 2026.
* The author is with the Department of Electrical Engineering and Information Technology, Iranian Research Organization for Science and Technology (IROST), Tehran, Iran.
E-mail: Moghaddam@irost.ir.
Corresponding Author: Majid Moghaddam.

instead to a broader spectrum of electricity generation sources notably renewable energy sources (RES) such as solar and wind. This bidirectional coupling between EVs and RES creates a unique opportunity to establish an integrated, sustainable, and flexible energy ecosystem. Its benefits extend far beyond transportation, with the potential to reshape the power industry and overall energy consumption patterns [1], [2].

The modern electric vehicle, distinct from its early predecessors, represents a sophisticated and intelligent propulsion system. It comprises high-efficiency electric motors, advanced power electronic converters, and battery packs with optimized thermal and electrical management. Beyond providing motive power, these technologies enable smart integration with modern transportation and energy grids, enhancing safety, traffic coordination, and overall system efficiency.

Challenges such as driving range limitations, lengthy charging times, and battery longevity concerns persist. Nevertheless, the rapid pace of innovation in core technologies points toward a bright future for widespread EV adoption. Within this context, the development of efficient, reliable, and user-friendly charging methods has become a cornerstone for the success of this transformation.

Figure 1 illustrates the core technological driver of EV adoption. There is a strong correlation between increasing battery range (the distance traveled on a single charge) and rising market share. The analysis of the chart data indicates a strong causal relationship [8]. Incremental advancements in battery energy density directly result in increased operational range for electric vehicles, which serves as the primary catalyst for widespread market adoption. Attaining a consistent driving range exceeding 1000 km on a single charge marks a technological transition that reshapes consumer priorities and shifts market demand toward electric vehicles. Consequently, charging infrastructure requirements must also evolve in parallel.

While conventional conductive charging methods satisfy the fundamental requirement for energy transfer, their inherent limitations specifically the need for manual intervention and the inability to charge in motion constitute a fundamental barrier to realizing a fully integrated and automated transportation ecosystem. Consequently, Wireless Power Transfer (WPT) technology emerges not as a mere alternative, but as an indispensable infrastructural prerequisite for the future of electric mobility. Hence, the projected dominance of electric vehicles by 2030–2035 is not merely a quantitative sales projection; it is clear evidence of the necessity for the parallel development, standardization, and commercialization of high-power, efficient, and robust WPT systems.

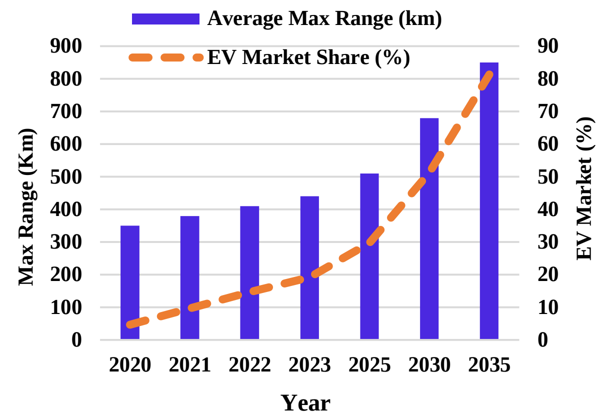

Fig.1. Key forecast data for global Electric Vehicle according to International Energy Agency (IEA) [8].

This study specifically addresses the design and development of a critical component within this forthcoming infrastructural requirement.

Research in WPT for electric vehicles is primarily directed at two fundamental approaches, radiative (far-field) and non-radiative (near-field) methods. For high-power, short-range applications such as EV charging, non-radiative methods are the focus of significant development. These are subdivided into two core physical principles: magnetic inductive coupling and electric capacitive coupling.

Magnetic inductive coupling enables power transfer via a time-varying magnetic field established between a pair of coupled inductors (coils). In contrast, electric capacitive coupling operates through a varying electric field generated between conductive plates.

For high-power applications like EV charging, magnetic inductive coupling presents distinct advantages and is the prevailing technology. A primary benefit is its robustness to environmental factors and non-metallic obstructions within the transfer path. Electric capacitive coupling, whereas theoretically viable, is constrained by significant practical limitations. Its efficiency is critically dependent on maintaining minimal distance and precise alignment between plates. As the operational air gap increases to the several centimeters required for vehicle charging, the effective coupling capacitance diminishes drastically, leading to a severe decline in power transfer efficiency [9]-[11].

The established technological solution for wireless EV charging is Resonant Inductive Power Transfer (RIPT). This method enhances basic inductive coupling by incorporating resonant circuits at both the transmitter and receiver, operating at a common high frequency, typically within the 81.39–90 kHz band as specified by key international standards such as SAE J2954 [9]. This resonant coupling enables highly efficient energy transfer. RIPT systems are capable of delivering power across a remarkable range, from milliwatts to hundreds of kilowatts, over a practical air gap. Consequently, it forms the technical foundation for both static and dynamic wireless charging (DWC) infrastructures for electric vehicles [13].

Radiative power transfer, in contrast to its inductive counterpart, operates through the emission and propagation of electromagnetic waves. Its efficacy is contingent upon the antenna dimensions being commensurate with the radiation wavelength, enabling electric charges to achieve the necessary acceleration for efficient radiation. In this regime, the transmitted power density attenuates proportionally to 1/r2, permitting energy transfer over considerable distances. Consequently, this technology is practical and prevalent at high frequencies (GHz range), where wavelengths are on the order of centimeters, allowing for compact antenna design. Conversely, at low frequencies (kHz range) and for short-range applications, the requisite antenna size becomes impractically large, and radiation efficiency diminishes drastically. Therefore, radiative transfer via antennas is ill-suited for such conditions, where inductive or resonant magnetic coupling methods present a far more efficient alternative for wireless power delivery.

Therefore, this manuscript focuses on the development of a high-efficiency Inductive Wireless Power Transfer (IWPT) system for electric vehicle charging, addressing the inherent limitations of radiative approaches for this high-power, short-range application.

The rest of this paper is organized as follows. section 2 reviews wireless power transfer technologies. Section 3 contains the design of a high-power misalignment-tolerant wireless charger. Section 4 describes the results and discussion and finally, Section 5 concludes the paper.

2 Review of Wireless Power Transfer Technologies

Wireless power transfer for electric vehicles (EVs) has emerged as a key technology to enhance user convenience and eliminate the limitations of physical-contact charging. Early literature in this field primarily focused on introducing and comparing different power transfer technologies. The study in [14] focused on the granular optimization of system components, with a detailed analysis performed on coil design and its impact on system efficiency. Employing an array of ferrite-core transmitter coils, the research investigated key parameters including turn count, inter-coil spacing, and mutual inductance, achieving a 20W transfer across a 2.5cm air gap in a controlled setting. Such investigations provide the essential groundwork for understanding and refining the core parameters that govern efficient power transfer.

Another stream of research in [15] successfully demonstrated the integration of photovoltaic sources with inductive WPT systems for EV charging. For instance, a design targeting 1 kW transfer across a 10cm gap achieved 90% efficiency in simulation. However, such systems often rely on standard two-coil (transmitter-receiver) architectures, which are fundamentally limited by their sensitivity to misalignment and rapid efficiency drop with increasing distance.

Reference [16] provided a comprehensive review of various methods, including radiative power transfer (such as microwave and laser) and near-field coupling techniques (inductive and capacitive). It ultimately identified Inductive Power Transfer (IPT) as the primary candidate for EV charging due to its advantages in safety, reliability, and high efficiency at significant power levels. This review also examined control systems, battery types, and their models, highlighting the inherent complexity of designing an integrated and efficient charging system.

A practical case study in this domain was presented by [17], which introduced a laboratory-scale system employing two receiver coils to enhance energy capture. The system operated at 50kHz, employing large-scale transmitter coils (0.5m outer diameter, 15 turns) embedded in the road with 1.5m spacing. The experimental evaluation compared single versus dual receivers at vehicle speeds of 10km/h and 100km/h. The results demonstrated a high output power of 4.8kW at 500 V with a notable efficiency of 90.2% under optimal conditions (dual receivers, 10km/h speed). However, a critical drawback was revealed like the required charging duration was impractically long (approximately 20 hours of continuous travel at 10 km/h for a full charge). This finding underscores an inherent compromise in contemporary DWC systems between optimizing power transfer efficiency under constraints and attaining practically useful energy transfer rates. Consequently, achieving such rates remains the foremost engineering challenge for making DWC a viable replacement for conventional conductive charging.

With the established superiority of inductive technology, research focus shifted towards its application in various charging modes, including DWC. The study by [18] specifically concentrated on optimizing efficiency in DWC systems, reaffirming the widespread use of inductive coupling and magnetic resonance methods. This research indicates that employing intermediate elements, such as relay coils, can enhance overall system efficiency.

In summary, whereas foundational progress in IPT is evident, a significant gap persists between laboratory-scale demonstrations and the stringent requirements for viable commercial deployment. Specifically, there is a pronounced lack of validated, high-power dynamic IPT systems that can simultaneously demonstrate robust efficiency, high misalignment tolerance, and long-term reliability. Therefore, achieving the high energy transfer rates necessary for practical rapid in-motion charging unequivocally necessitates a breakthrough in system architecture and a substantial increase in operational power level. This work aims to address this critical gap through a novel design and comprehensive simulation study of an advanced IPT system. The proposed architecture is explicitly designed to fulfill these paramount requirements, providing a theoretical and simulated foundation for future experimental validation.

3 Design of a High-power Misalignment-Tolerant Wireless Charger

The literature review has established the need for high-power dynamic wireless charging systems that maintain efficiency under real-world conditions. In response, this section introduces the proposed system architecture, detailing the design of its core components, the power converter topology, the coupler (coil) assembly, and the control strategy. The design of an efficient wireless charger for electric vehicles requires careful selection and integration of power electronic converter stages. This section outlines the proposed system architecture, beginning with a review of common converter topologies to justify the chosen design.

Various power electronic converters are employed in EV chargers, including AC-DC, DC-AC, DC-DC, and AC-AC types, each serving specific functions. Studies on EV charger topologies indicate that a conventional charger typically comprises a front-end AC-DC converter followed by a back-end DC-DC converter [19]. Modern chargers are designed to achieve Active Power Factor Correction (PFC) using Buck or Boost converter topologies.

In EV charger structures, diode bridge rectifiers are widely used for AC to DC conversion. However, these uncontrolled rectifiers inject significant harmonics into the grid. Drawbacks such as non-sinusoidal input current, output voltage harmonics, low input power factor, and unidirectional power flow have motivated recent research to replace them with controlled active rectifiers. To mitigate harmonic-related issues, active rectifiers, current filters, or dedicated PFC circuits are employed.

Current filters (AC filters), constructed using inductors (L), capacitors (C), or their combinations (LC or LCL), are essential. Due to the presence of large capacitors on the DC side, limiting the current transient on the AC side is necessary. The primary objectives of these filters are to improve input current quality and limit inrush current. For low-power applications with high switching frequencies, an input capacitive filter may also serve this purpose.

The rectified input power must be conditioned to appropriate voltage and current levels for battery charging, a task performed by the subsequent converter stage. The transfer of power from the grid to the battery commonly involves two converter stages, known as two-stage power conversion. Whereas, single-stage conversion is possible, for high-power transfer, only a two-stage power electronic architecture is feasible. Furthermore, two-stage chargers exhibit lower fluctuations in output voltage or current.

Increasing the switching frequency presents advantages for high-power transfer and reduces the physical size of inductive and capacitive components. However, operating at excessively high frequencies introduces significant challenges related to Electromagnetic Interference (EMI) emission. Elevated dv/dt and di/dt rates can generate substantial interference with the grid and adjacent equipment. Suppressing this interference requires the implementation of a sizable and complex EMI filter at the converter input, which in turn increases the overall converter volume. This presents a notable design constraint for high-power systems. Consequently, determining an optimal switching frequency constitutes a critical design trade-off, underscoring the necessity of a carefully optimized design.

The second stage of the EV charger features a DC-DC converter to regulate the voltage and current injected into the battery. Various charging profiles have been established for optimal battery charging. The inclusion of voltage and current control loops within the DC-DC converter enables the implementation of these diverse charging patterns. Harmonics in the output voltage and current can increase battery temperature, raise losses, and consequently reduce battery lifespan. Therefore, an output filter is placed between the charger output and the battery input [2].

The overall architecture of the proposed charger, integrating the components and considerations discussed in this section, is presented in Fig. 2. The input PFC stage interfaces the system with the three-phase AC grid. A front-end EMI filter suppresses high-frequency switching noise. This is followed by a three-phase diode bridge rectifier, which converts the AC voltage to DC. The cornerstone of this stage is an active PFC converter, typically implemented as a boost topology. Its dual function is to shape the input current waveform for a near-unity power factor and to provide a stable, regulated DC link voltage (600 V) for the subsequent high-power stage. The stable DC voltage is then converted into a high-frequency AC signal by a full-bridge H-bridge inverter operating at the system's

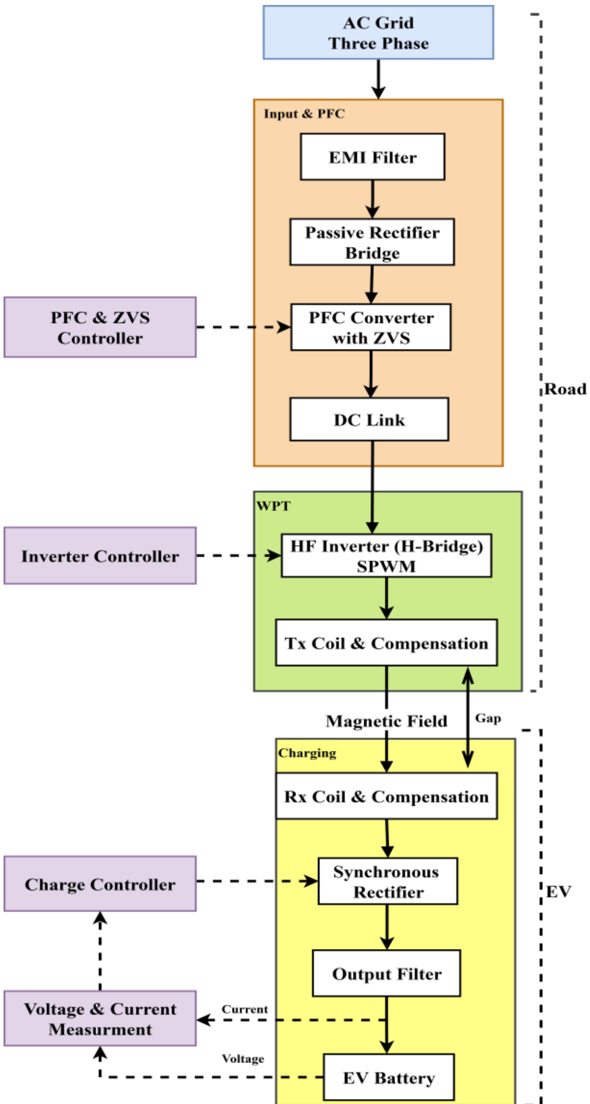

Fig.2. Proposed system architecture for wireless charging of Electric Vehicles.

resonant frequency (100 kHz). The inverter output feeds a primary-side series compensation network, which cancels the inductive reactance of the transmitter coil, maximizing the current and establishing a strong oscillating magnetic field.

The core of WPT stage performs the conversion from electrical to magnetic energy. Energy is coupled across the 10 cm air gap via magnetic resonance to the vehicle-side receiver coil. After passing through its dedicated secondary series compensation network, the received AC power is rectified back to DC by a high-frequency synchronous rectifier (a full MOSFET bridge).

The output regulation and battery charging stage, located on the vehicle, conditions the received power for the battery. The rectified DC is smoothed by an output LC filter. The synchronous rectifier directly provides the regulated DC voltage required for battery charging. It regulates the output to follow standard Constant Current/Constant Voltage (CC/CV) charging profiles, provides galvanic isolation for safety, and delivers power at the required voltage level to the EV battery pack.

The control system ensures stable power transfer and safe battery charging through a dedicated manual control algorithm. This algorithm measures the battery terminal voltage and the charging current (via sensors placed before the battery). It implements the CC/CV algorithm by adjusting the gate signals of the synchronous rectifier. This hardware-based control strategy, implemented with analog comparators and timing logic, ensures stable and safe charging without requiring a complex digital processor.

The voltage equations for the primary and secondary sides of the proposed series-series compensated WPT system are expressed as:

$$V_1 = \left(R_1 + j\omega L_T + \frac{1}{j\omega C_P}\right) I_1 + j\omega M I_2 \tag{1}$$

$$V_2 = \left(R_2 + j\omega L_R + \frac{1}{j\omega C_S} + R_L\right) I_2 + j\omega M I_1 \tag{2}$$

In these equations, V_1 and V_2 represent the primary and secondary coil voltages, while I_1 and I_2 are the corresponding currents. The self-inductances of the transmitter and receiver coils are denoted by L_T and L_R, with their respective series resistances $R_1$and R_2. The compensation capacitors C_T and C_R are connected in series with the coils to achieve resonance at the operating frequency of 100 kHz.

The mutual inductance between the two coils is given by:

$$M = K\sqrt[2]{L_T L_R} \tag{3}$$

where k is the coupling coefficient ($0 < k < 1$), which depends on the coil geometry and the 10 cm air gap. For the ferrite-core configuration, a higher k value is achieved due to the low-reluctance magnetic path.

Under resonance conditions, where $\omega L_T = 1/(\omega C_T)$ and $\omega L_R = 1/(\omega C_R)$, the maximum power transferred to the load can be derived as:

$$P\_Max = \frac{V_1^2\, \omega^2\, M^2\, R_L}{[R_1(R_2 + R_L) + \omega^2\, M^2]^2} \tag{4}$$

This equation demonstrates that the power transfer capability is strongly dependent on the mutual inductance M, the operating frequency ω, and the load resistance R_L. At the designed resonance frequency of

100 kHz, with the ferrite-core configuration achieving a high mutual inductance, the system is capable of transferring 2.4 kW to the battery. The optimal load resistance for maximum power transfer can be obtained by differentiating this expression with respect to R_L.

The coil-to-coil efficiency of the WPT system under resonance conditions is expressed as:

$$\eta = \frac{R_L\,\omega^2 M^2}{(R^2 + R_L)[R_1(R_2 + R_L) + \omega^2 M^2]} \qquad (5)$$

The equation shows that efficiency improves with higher mutual inductance M and optimal load resistance R_L.

A detailed parametric design of a wireless charging system is described here. The details of the parametric design and calculations for each stage of the charging system is presented. The proposed system topology is illustrated in Fig. 3, which shows the complete power conversion chain from the three-phase AC input to the EV battery.

The objective is to convert a 380V three-phase AC industrial supply into a controlled power source suitable for efficiently and safely charging the target electric vehicle battery through a 10cm air-gap via resonant inductive coupling. The system begins with a three-phase AC input of 380V line-to-line at 50 Hz. The AC voltage is then rectified to DC using a three-phase bridge. The theoretical average DC voltage at this point is approximately 513V, which in practice reduces to about 510V after accounting for diode forward voltage drops. This voltage is fed into an active PFC boost converter. The PFC stage serves the dual purpose of drawing a sinusoidal current from the grid with a near-unity power factor and boosting the DC voltage to a stable 600V level required for the high-frequency inverter. The required boost converter duty cycle for this step-up is calculated to be approximately 15%. A boost inductor of 120µH is selected to limit current ripple, while a DC-link capacitor bank with an effective capacitance of 350µF is designed to minimize voltage ripple on the 600V bus.

The 600V DC is converted to high-frequency AC by a full-bridge (H-Bridge) inverter. The inverter employs Sinusoidal Pulse Width Modulation (SPWM) to generate a quasi-sinusoidal output with its fundamental frequency precisely controlled at 100kHz.

The inverter output drives the primary side of the wireless link, which consists of a series compensation network and the transmitter coil. The air-cored transmitter coil is designed with 50 turns of Litz wire, resulting in an inductance (L_T) of 150µH.

A series compensation capacitor (C_T) of 16.9nF is tuned to form a resonant tank at 100kHz with L_T. On the vehicle side, the receiver coil is similarly air-cored and features 150 turns wound in two series layers, yielding an inductance (L_R) of 600 µH. Its series compensation capacitor (C_R) is 4.2nF.

The AC voltage induced in the receiver coil is first rectified using a high-efficiency synchronous rectifier based on low-R_{ds}(ON) MOSFETs to minimize conduction losses. To provide a safe path for reverse and freewheeling currents, ultrafast recovery diodes are connected in parallel with each power MOSFET (see in Fig. 3). These diodes prevent destructive voltage spikes and improve overall system robustness. At the output of the synchronous rectifier, a second-order low-pass LC filter is employed to attenuate the high-frequency switching ripple (100 kHz). The filter consists of a series inductor L_f = 60 µH and a parallel capacitor C_f = 100 µF. The inductor limits the current ripple, while the capacitor stabilizes the output voltage, providing a clean DC input to the battery charger. The cutoff frequency of the filter is designed to be well below 100 kHz to ensure effective ripple suppression without affecting the DC component.

In practice, to effectively attenuate the high-frequency switching ripple (100 kHz), the output capacitor C_f is implemented as a parallel combination of a 100 µF electrolytic capacitor (for bulk energy storage and low-frequency filtering) and a 1 µF ceramic capacitor (for high-frequency decoupling). This is a standard design practice in switching power supplies to ensure a clean DC voltage for the battery charger. This DC voltage is then directly applied to the battery pack.

The charging process follows a constant-current/constant-voltage (CC/CV) algorithm. A dedicated control circuit (implemented with analog comparators, voltage references, and timing logic) measures the battery terminal voltage and the charging current via sensors placed before the battery. It directly adjusts the gate signals of the synchronous rectifier to regulate the output, during the CC phase the charging current is kept at the desired level (≈12 A), and when the battery voltage reaches 200 V the algorithm switches to the CV phase, holding the voltage constant while allowing the current to taper off. No isolated DC-DC converter is used; the synchronous rectifier directly provides the required 200 V DC.

Table 1 summarizes the main components of the power electronic converters employed in the proposed wireless charging system. All components are labelled consistently with the circuit schematic of Fig.3. The component values and ratings are derived from the design specifications and simulation setup described in Section 4. The selected parts are suitable for 100 kHz operation and meet the voltage and current requirements of the 2.4 kW dynamic charging system.

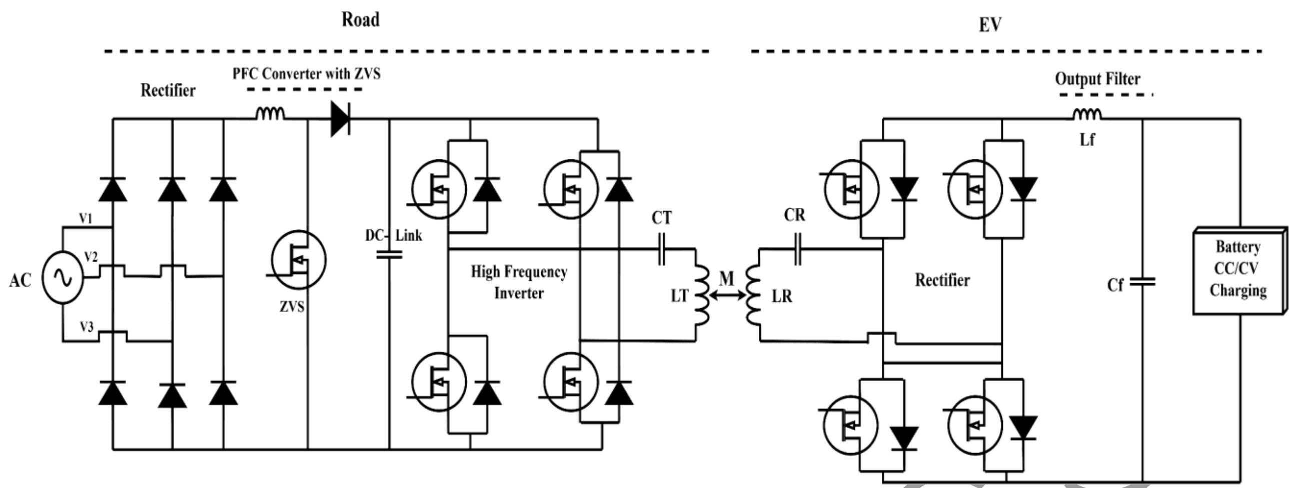

Fig. 3. Proposed topology of the inductive wireless power transfer system with series-series (S/S) resonant compensation. The system includes a three-phase AC input, ZVS rectifier, PFC boost converter, H-bridge inverter (SPWM at 100 kHz), ferrite-core coils with 10cm air gap, synchronous rectifier, output LC filter for CC/CV battery charging.

Table 1. Component specifications of the power electronic converters.

Component	Symbol	Value	Description
Three-phase AC input	AC	380 V (line-to-line), 50 Hz	Industrial supply
Diode bridge rectifier	D1–D6	fast recovery diode	PSD86-12 (1200V, 86A, three-phase bridge module)
Boost inductor (PFC)	L_boost	70 µH	15 A, low DC resistance
PFC MOSFET	M_PFC	MOSFET	1200 V, 30 A, R_{ds}(on) = 80 mΩ, ZVS operation
PFC fast diode	D_PFC	Diode	1200 V, 10 A
Capacitor bank	DC_Link	200 µF, 630 V	low ESR, electrolytic
H-bridge inverter	M1-M4	MOSFET	1200 V, 30 A, Rds(on) = 80 mΩ, at 100 kHz
Primary compensation	C_T	27 nF	1 kV, tuned with L_T at 100 kHz
Transmitter coil (Tx)	L_T	150 µH	Litz wire, ferrite core, 50 turns
Receiver coil (Rx)	L_R	600 µH	Litz wire, ferrite core, 150 turns (double layer)
Secondary compensation	C_R	4.2 nF	1 kV, tuned with L_R at 100 kHz
Synchronous rectifier	M5-M8	MOSFET	55 V, 49 A, R_{ds}(on) =17.5 mΩ;
Output filter inductor	L_f	60 µH	Powder iron core, 15 A, low loss
Output filter capacitor	C_f	100 µF / 250 V electrolytic + 1 µF / 250 V ceramic	Parallel combination
Battery pack	Batt	200 V, 13.2 Ah, 2.64 kWh	48 cells in series, 6 parallel strings (2.2 Ah per cell)

4 Results and Discussions

This study employed two distinct design scenarios to model and optimize the WPT system for dynamic electric vehicle charging. The primary objective was to evaluate core material selection's impact on coupling efficiency, electromagnetic performance, and practical feasibility. The first scenario utilized an air-core configuration for both transmitter (Tx) and receiver (Rx) coils. The geometry was optimized based on practical constraints: the Tx coil, embedded in the road, was designed with 50 turns, while the under-vehicle Rx coil featured 150 turns arranged in a double-layer winding to maximize flux capture within a limited space. Both coils were wound with 1.5 mm diameter copper wire with minimal inter-turn spacing.

A critical air gap of 10 cm was maintained, representing the clearance between the road surface and the vehicle underbody. Figure 4 depicts the balanced three-phase AC input voltage source applied to the system, illustrating its defined amplitude (380 V line-to-line RMS, peak ≈311 V), frequency (50 Hz), and 120-degree phase displacement. Figure 5 presents the output of the three-phase diode bridge rectifier in Scenario 1 (air-core configuration), which is a pulsating DC voltage with a peak-to-peak ripple of approximately 72 V (13.4%), varying between 463 V and 535 V. This waveform serves as the input to the PFC boost converter in the subsequent stage.

Figure 6 presents the magnetic field and flux lines for the air-core design (Scenario 1). The resulting field distribution exhibits significant dispersion, highlighting the need for improved flux guidance, which is addressed in the subsequent design by incorporating a ferrite core. Furthermore, the open-circuit voltage induced in the secondary coil is shown in Fig. 7. As expected from the turns ratio, this induced voltage reaches a peak of approximately 700 V. However, a significant voltage drop was observed at the secondary coil upon load connection, indicating an inefficient flux path and low coupling efficiency, which are inherent limitations of air-core designs.

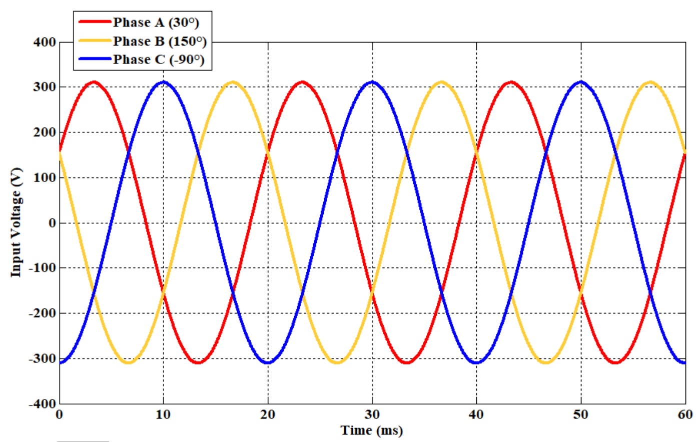

Fig. 4. The three-phase input voltage signals with their specific amplitude, frequency, and phase relationships.

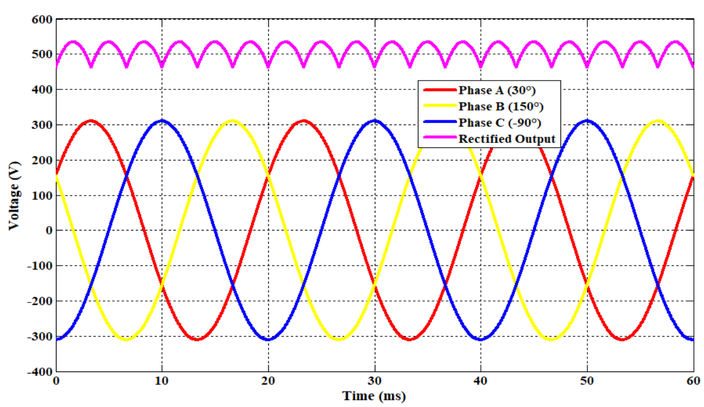

Fig. 5. Three-phase rectifier output voltage with a peak-to-peak ripple of approximately 72 V, varying between 463 V and 535 V.

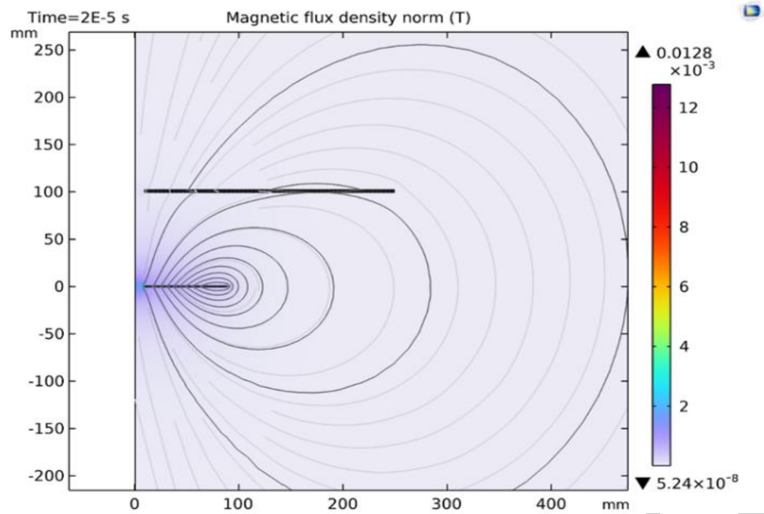

Fig. 6. The magnetic field and flux lines for the air-core design.

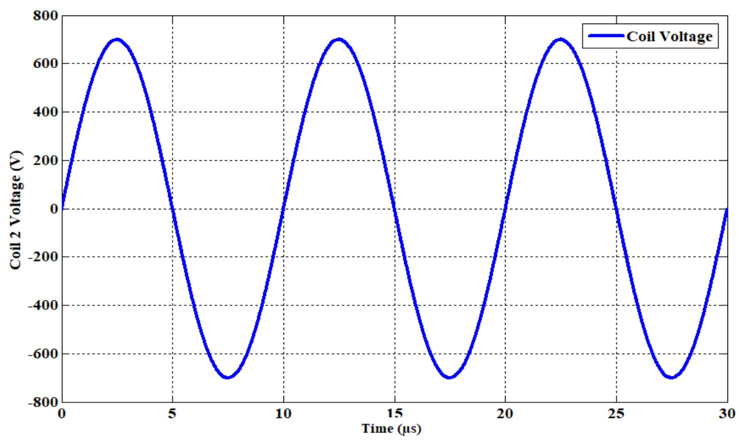

Fig. 7. The open-circuit voltage induced in the secondary coil with air core under no-load conditions.

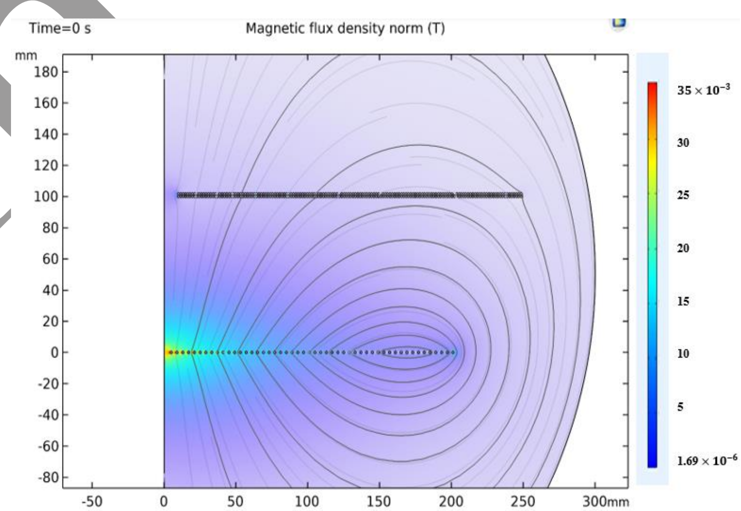

Fig. 8. Two-dimensional magnetic field distribution and flux lines for the ferrite-core configuration obtained from COMSOL simulation.

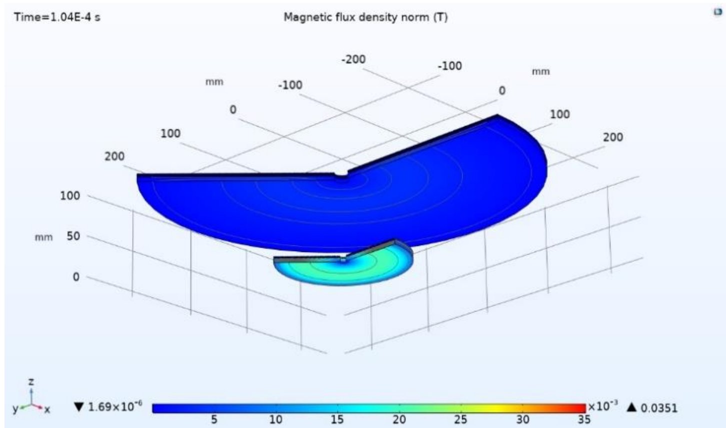

Fig. 9. The three-dimensional magnetic field distribution and flux lines for the ferrite-core configuration obtained from COMSOL simulation.

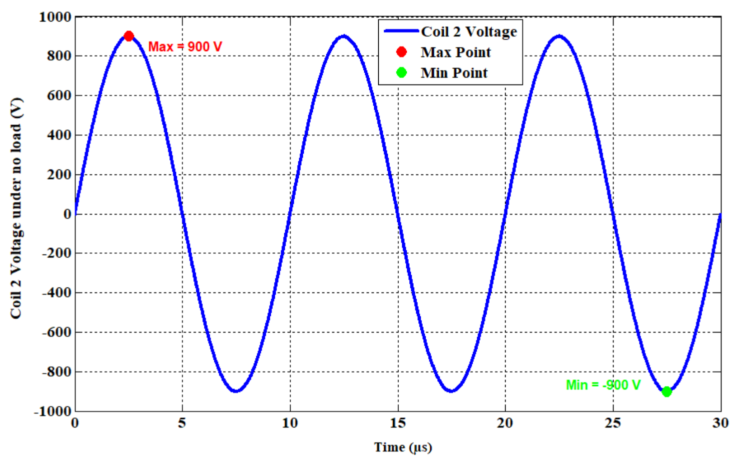

Fig. 10. Induced voltage in the secondary coil with ferrite core under no-load conditions (f = 100 kHz, V_peak ≈ 900 V).

To address this limitation, Scenario 2 was proposed, focusing on enhancing the magnetic circuit. The primary coil was redesigned with an increased pitch—specifically, a 4 mm center-to-center distance. This modification effectively widened its area while maintaining the same number of turns, thereby improving flux coverage. More critically, strategic placement of ferrite cores was introduced. These cores were positioned around the primary coil's periphery, at its center, and on its underside to create a preferential, low-reluctance path for the magnetic flux. This design directs the flux more effectively toward the receiver. The simulation results for this enhanced configuration confirm a substantial improvement.

The improved magnetic field distribution and flux lines, achieved by incorporating the ferrite core and the three-dimensional of that obtained from COMSOL Multiphysics simulations, are shown in the Fig. 8 and Fig. 9 respectively. The magnetic field and flux line diagrams reveal superior flux concentration and linkage. Also, the induced voltage on the secondary coil is demonstrated in Fig. 10. Consequently, the induced voltage on the secondary coil shows a notable increase of 200 V at its peak compared to the air-core scenario. This improvement directly translates to a higher power transfer capability and greater resilience against voltage droop under no load condition.

Figure 11 presents the secondary coil voltage under load conditions, contrasting with the open-circuit voltage shown in Fig. 10. In conclusion, the comparative analysis validates that whereas a basic air-core system is functional, its performance is limited by poor magnetic coupling.

The proposed enhanced design characterized by a widened primary coil pitch and strategic ferrite core placement effectively resolves these issues. It markedly improves flux linkage and magnetic coupling, which in turn elevates the induced secondary voltage and yields a more robust, load-tolerant WPT system ideally suited for dynamic EV charging. Notably, the simulation results highlight a fundamental engineering trade-off: while the air-core variant avoids core losses and reduces material costs, its low coupling coefficient severely limits performance. In contrast, the ferrite-core design, despite incurring slightly higher material expenses, delivers a superior equilibrium between efficiency, power transfer capability, and practical resilience, thereby confirming its suitability for real-world dynamic charging applications.

The performance of the front-end PFC stage is evaluated in terms of voltage regulation and input current quality. Figure 12 demonstrates the output of the three-phase diode bridge rectifier, which is a pulsating DC voltage with a peak-to-peak ripple of approximately 72 V (13.4%), varying between 463 V and 535 V. This waveform serves as the input to the PFC boost converter. Figure 13 compares the rectified DC voltage (input to the PFC) with the regulated DC link voltage (output of the PFC). The PFC stage successfully boosts and stabilizes this voltage to a nominal value of 600 V with a peak-to-peak ripple of approximately 9 V (1.5%), confirming the effectiveness of the closed-loop voltage regulation. This significant reduction in ripple (from 13.4% to 1.5%) ensures a stable and clean DC bus for the downstream inverter, minimizing stress on the switching devices and improving overall system reliability.

Figure 14 compares the three-phase AC input current drawn from the grid before and after PFC activation. Without PFC, the current is severely distorted with significant harmonic content, resulting in a low power factor of approximately 0.72. After PFC activation, the current becomes sinusoidal and in phase with the grid voltage, achieving a near-unity power factor (≈0.99). This improvement directly reduces the RMS current drawn from the grid for the same power delivery, thereby lowering conduction losses and stress on the upstream network. This confirms the dual role of the PFC stage, providing a stable DC bus and improving the input power quality.

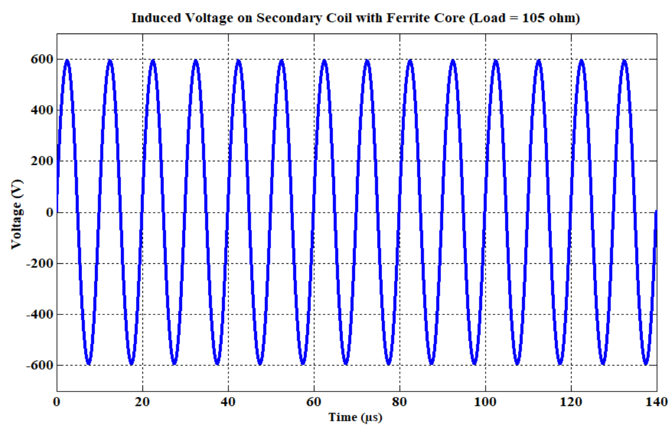

Fig. 11. The induced voltage on the secondary coil with ferrite core under load conditions.

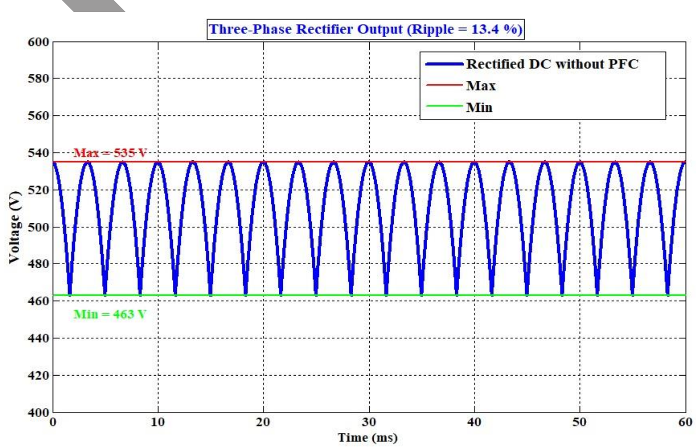

Fig. 12. Three-phase rectifier output voltage with a ripple of approximately 13.4% (463–535 V).

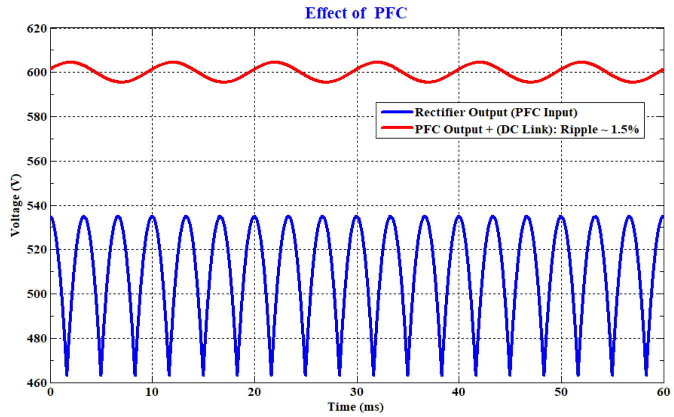

Fig. 13. Comparison of the rectifier output (input to PFC) and the regulated DC link voltage after PFC (600 V with ripple 1.5%).

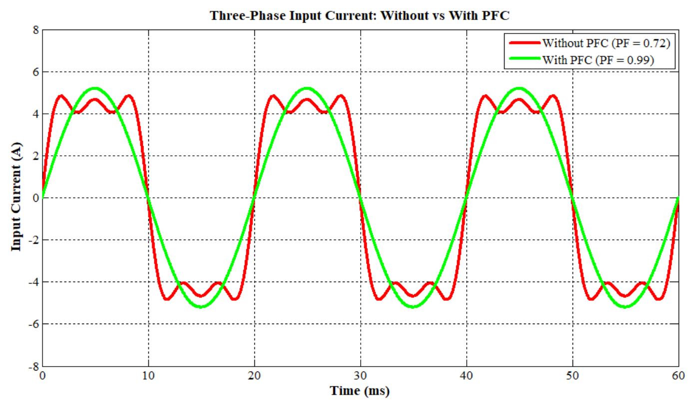

Fig. 14. Three-phase input current waveform without and with PFC, showing the improvement in power quality and power factor.

The implemented charging algorithm for the 48S6P battery pack (48 cells in series, 6 strings in parallel; nominal 200 V, 2.4 kW according to Eq. 6) follows a combined constant-current/constant-voltage (CC/CV) method. This choice was made after a comparative simulation study of several charging strategies (constant-voltage, pulsed square-wave, variable-current), which showed that the constant-current method required the shortest charging time up to approximately 83 % of the final state of charge (SOC). As shown in Fig. 15, the process begins with a CC phase at ≈12 A (Simcenter Amesim was used for battery pack design). During this phase, the pack voltage rises linearly. A current sensor placed after the LC filter and before the battery measures the charging current, while a voltage sensor connected across the battery terminals monitors the voltage. Both sensors feed a hardware control circuit (analog comparators, voltage references, timer logic that directly adjusts the gate signals of the synchronous rectifier MOSFETs (M5–M8). No digital processor is used; the control is purely hardware-based. When the pack voltage reaches ≈200 V (at ≈3000 seconds, with SOC near 80 %), the circuit automatically switches to the CV phase: the voltage is held constant at ≈200 V, and the charging current tapers off exponentially until it falls below a predefined cut-off threshold. This CV phase safeguards the battery against overvoltage and lithium plating – primary causes of capacity fade and reduced cycle life. The combined CC/CV strategy thus provides an optimal charging process for the wireless power transfer system.

$$200_{\text{pack voltage}} = N_{\text{number of series cell}} \times 4.2_{\text{cell voltage}} \Rightarrow N = 48 \quad (6)$$

Among the systems compared in Table 2, the proposed design is the only one that demonstrates quantified practical dynamic charging capability for passenger electric vehicles. References [20]– [22] are exclusively designed for stationary (static) charging and do not address in-motion operation. Although the system by [17] claims dynamic charging ability, its reported performance is highly impractical, requiring 20 hours and 833 km to fully charge the battery at 10 km/h.

The system by [23] is a dynamic capacitive power transfer (DCPT) system, but it is specifically designed for tramway (rail) applications, not for passenger EVs, and thus is not directly comparable. In contrast, the proposed system achieves a full dynamic charge in only 3.125 hours over a distance of 31.25 km at the same speed. Furthermore, the proposed system achieves a coil-to-coil efficiency exceeding 96% at a realistic 10 cm air gap and maintains stable operation under lateral misalignments ($\eta > 80\%$ up to ± 10 cm), demonstrating its practical superiority beyond dynamic charging capability.

This clearly shows that the proposed system offers a realistic and feasible solution for road-embedded wireless charging infrastructure, whereas the other references either ignore dynamic operation, report impractical numbers, or target different transportation domains.

At first glance, the nominal power of 2.4 kW may seem lower than the 3 kW, 4.8 kW, and 5 kW of other references. However, this power level is deliberately chosen as the optimal sweet spot for dynamic on-road charging. A lower power reduces current, which directly lowers ohmic losses, simplifies thermal management, and increases overall system reliability while cutting manufacturing and installation costs. Therefore, the 2.4 kW power rating is not a drawback but an intentional, well-justified engineering choice for practical dynamic EV charging.

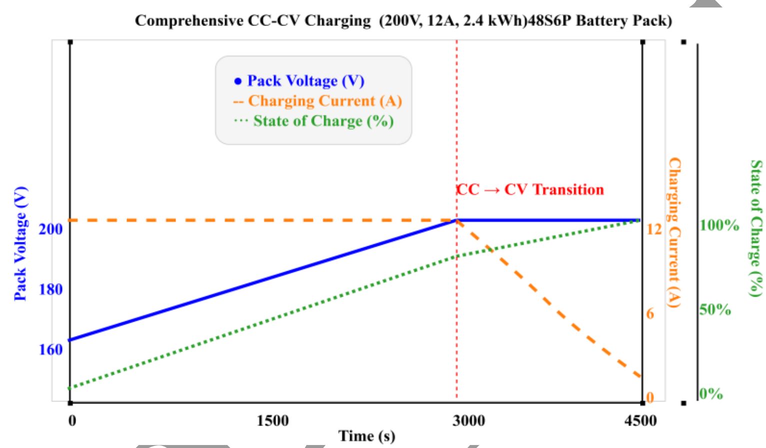

Fig. 15. The implemented charging algorithm for the battery pack (comprising 48 cells in series and 6 strings in parallel).

Table 2. Performance comparison of the proposed DWC system with state-of-the-art EV wireless charging systems (2022–2026). Note: N/A indicates "Not Applicable", meaning that the corresponding system is not designed for dynamic charging.

Parameter	Proposed (This work)	Ref. [17] (2022)	Ref. [20] (2026)	Ref. [21] (2025)	Ref. [22] (2025)	Ref. [23] (2025)
Technology	Inductive	Inductive	Inductive	Inductive	Inductive	Capacitive
Compensation topology	S/S + Ferrite	S/S, Air-core	S/S, Air-core	Double-sided LCC	Multiphase parallel-connected	Four vertical plates
Charging type	Dynamic/Static	Dynamic/Static	Static	Static	Static	Dynamic (tramway)
Nominal power (kW)	2.4	4.8	5	3.0	1.4	2.76
Frequency	100 kHz	50 kHz	85 kHz	85 kHz	85 kHz	1MHz
Max efficiency (static, %)	>96%	90.2% (no-load)	88.4%	95.47%	93.53%	92.6%
Air gap (cm)	10	10	1	15	10	10
Misalignment tolerance (static)	~10 cm (η>80%)	Low (air-core)	Sharp drop at 6 cm	15 cm	10 cm (η>80%)	N/A (rail system)
Time for full dynamic charge at 10 km/h (h)	3.125	20	N/A (Static)	N/A (Static)	N/A (Static)	N/A (Tramway)
Distance for full dynamic charge at 10 km/h (km)	31.25	833	N/A	N/A	N/A	N/A

5 Conclusion

This study successfully designed, simulated, and validated a high-efficiency inductive Wireless Power Transfer (WPT) system, establishing a critical foundation for the development of Dynamic Wireless Power Transfer (DWPT) for electric vehicles. The proposed system architecture was engineered to manage the complete power conversion chain. It began with a three-phase AC input, which was converted to a regulated 600V DC bus via a three-phase diode bridge rectifier followed by an active PFC boost converter with zero-voltage switching (ZVS). At the heart of the system, an H-bridge inverter employing Sinusoidal Pulse Width Modulation (SPWM) operated at an optimized frequency of 100 kHz to drive the primary coil. Through rigorous simulation and modeling of both air-core and ferrite-core configurations, the critical role of magnetic design was quantified.

The simulation results conclusively demonstrated the system's high performance. With a 10cm air gap, representative of the distance between the road and the vehicle underbody, the ferrite-core configuration achieved a coil-to-coil power transfer efficiency exceeding 96%, a dramatic improvement over the air-core design. This high-efficiency transfer enabled the wireless delivery of 2.4 kW of power, which was subsequently conditioned by a synchronous rectifier and an LC output filter to provide a stable 200V output suitable for constant-current/constant-voltage (CC/CV) EV battery charging. In conclusion, this work validated the technical feasibility of in-motion wireless charging by demonstrating that high-efficiency power transfer was achievable with an optimized magnetic circuit design. The significant performance gain observed with ferrite cores underscored magnetic flux confinement as a non-negotiable requirement for practical, real-world WPT systems.

Future work should focus on experimental validation of the proposed ferrite-core dynamic charging system under real-road conditions, including varying vehicle speeds, lateral misalignments, and environmental factors such as moisture and debris. Additionally, the integration of multi-coil transmitter arrays and intelligent power management strategies should be investigated to improve power continuity and ensure smooth switching between consecutive coils. Ultimately, this work provides a pathway to the practical deployment of dynamic wireless charging infrastructure.

Conflict of Interest

The authors declare no conflict of interest.

Author Contributions

The author is the sole contributor to this work and is responsible for all aspects of the research, including conceptualization, methodology, simulation, analysis, and manuscript preparation.

Acknowledgment

The author gratefully acknowledges the Iranian Research Organization for Science and Technology (IROST) for providing the necessary research facilities and administrative support during the course of this work.

Funding

No funding was received for this work.

Declaration of generative AI and AI-assisted technologies

The author declare that no generative AI or AI-assisted technologies were used in the writing process of this manuscript.

References

[1]. S. Wang and D. Dorrell, "Review of wireless charging coupler for electric vehicles," in IECON 2013-39th Annual Conference of the IEEE Industrial Electronics Society, IEEE, pp. 7274-7279. 2013.

[2]. F. Musavi, M. Edington, and W. Eberle, "Wireless power transfer: A survey of EV battery charging technologies," in 2012 IEEE Energy Conversion Congress and Exposition (ECCE), IEEE, pp. 1804-1810, 2012.

[3]. M. Moghaddam, M. H. Moaiyeri and M. Eshghi, "Design and Evaluation of an Efficient Schmitt Trigger-Based Hardened Latch in CNTFET Technology," in IEEE Transactions on Device and Materials Reliability, vol. 17, no. 1, pp. 267-277, 2017.

[4]. M. Moghaddam, S. Timarchi, M.H. Moaiyeri, and M. Eshghi, "An Ultra-Low-Power 9T SRAM Cell Based on Threshold Voltage Techniques. Circuits Syst Signal Process, Vol. 35, pp. 1437–1455, 2016.

[5]. M. Moghaddam, Z. Taghavi, "Dual-VDD System Design with Energy Efficient Near-Threshold Voltage Level Converter", International Journal of Nanoscience and Nanotechnology, Vo. 18, no. 1, pp. 55-64, 2018.

[6]. IEA, "Global EV Outlook 2025," International Energy Agency, Paris, France, 2025. [Online]. Available: https://www.iea.org/reports/global-ev-outlook-2025.

[7]. A. Zentani, A. Almaktoof, and M. T. E. Kahn, "A comprehensive review of developments in electric vehicles fast charging technology," Applied Sciences, vol. 14, no. 11, 2024.

[8]. International Energy Agency (IEA), "Global EV Outlook 2024", https://www.iea.org/reports/global-ev-outlook-2024.

[9]. G. A. Covic and J. T. Boys, "Inductive power transfer," Proc. IEEE, vol. 101, no. 6, pp. 1276–1289, Jun. 2013.

[10]. J. Huh, S. W. Lee, W. Y. Lee, G. H. Cho, and C. T. Rim, "Narrow-width inductive power transfer system for online electrical vehicles," IEEE Transactions on Power Electronics, vol. 26, no. 12, pp. 3666-3679, 2011.

[11]. C.-S. Wang, O. H. Stielau, and G. A. Covic, "Design considerations for a contactless electric vehicle battery charger," IEEE Transactions on industrial electronics, vol. 52, no. 5, pp. 1308-1314, 2005.

[12]. S. Li, W. Li, J. Deng, T. D. Nguyen, and C. C. Mi, "A double-sided LCLC compensation network and its tuning method for wireless power transfer," IEEE Trans. Veh. Technol., vol. 64, no. 6, pp. 2261–2273, Jun. 2015.

[13]. G. A. Covic, J. T. Boys, M. L. Kissin, and H. G. Lu, "A three-phase inductive power transfer system for roadway-powered vehicles," IEEE Transactions on Industrial Electronics, vol. 54, no. 6, pp. 3370-3378, 2007.

[14]. X. Zhang, Z. Yuan, Q. Yang, Y. Li, J. Zhu and Y. Li, "Coil Design and Efficiency Analysis for Dynamic Wireless Charging System for Electric Vehicles" IEEE Transactions on Magnetics, vol. 52, no. 7, pp. 1-4, July 2016.

[15]. M. Elwalaty, M. Jemli and H. B. Azza, "A Two-Rectangular Coils Wireless Charging Electric Vehicle with Photovoltaic Generator," 2019 19th International Conference on Sciences and Techniques of Automatic Control and Computer Engineering (STA), Sousse, Tunisia, pp. 455-460, 2019.

[16]. M. Amjad, M. Farooq-i-Azam, Q. Ni, M. Dong, and E. A. Ansari, "Wireless charging systems for electric vehicles," Renewable and Sustainable Energy Reviews, vol. 167, pp. 1-21, 2022.

[17]. N. Mohamed, A. Flah, M. Alqarni, R. A. Turky, B. Alamri, Z. M. Ali, and S. H. E. Abdel Aleem, "A new wireless charging system for electric vehicles using two receiver coils," Ain Shams Engineering Journal, vol. 13, no. 2, pp. 1-15, 2022.

[18]. S. S. Premarathna and V. Viswambaran, "Optimizing Efficiency in Motion: Dynamic Wireless Charging Systems for Electric Vehicles," Advances in Science and Engineering Technology International Conferences (ASET), Abu Dhabi, United Arab Emirates, 2024, pp.1-8, 2024.

[19]. R. L. Steigerwald, "A comparison of half-bridge resonant converter topologies," IEEE transactions on Power Electronics, vol. 3, no. 2, pp. 174-182, 1988.

[20]. I. A. Ayoade, O. M. Longe, "Design and experimental analysis for a high-power wireless charging system design for electric vehicles," Frontiers in Future Transportation, vol. 7, Jan. 2026.

[21]. T. S. Hassan, M. M. Z. Moustafa, and N. H. Abbasy, "High-Efficiency Wireless Power Transfer for Electric Vehicles: A Coil Geometry and PSO-Based Optimization Framework," IEEE Access, vol. 13, pp. 132952–132972, 2025.

[22]. W. Pan, Z. Shen, X. Yu, R. Xie, F. Zheng, X. Chen, X. Mao, and Y. Zhang, "An Adaptive and Scalable Wireless Charging System for Electric Vehicles with Enhanced Interoperability and Misalignment Tolerance," IEEE Transactions on Power Electronics, vol. 40, no. 11, pp. 14159–14168, Nov. 2025.

[23]. S. Kodeeswaran, M. Nandhini Gayathri, A. Kannabhiran, S. Padmanaban, and P. Carbone, "An Electrified Tramway Wireless Charging System for Rail Transportation Using Dynamic Capacitive Power Transfer with Four Vertical Plates," IEEE Transactions on Transportation Electrification, vol. 11, no. 3, pp. 7786–7797, Jun. 2025.

Majid Moghaddam received his Ph.D. in Electronics Engineering from Shahid Beheshti University, Tehran, Iran, in 2017. He is currently a faculty member at the Electrical and Information Technology Research Institute, Iranian Research Organization for Science and Technology (IROST), Tehran, Iran. He received the National Elite Foundation Award as a Distinguished Talent. His current research focuses on wireless power transfer systems for electric vehicle charging, alongside his broader interests in hardened low-power circuit and system design, energy-efficient storage cell design, and fault-tolerant electronic architectures. He has published numerous papers in reputable international journals and has led several industrial projects focused on low-energy consumption and high-performance electronic systems.